RESEARCH ARTICLE

Changes in neurological and pathological outcomes in a modified rat spinal cord injury model with closed canal

Xin Sun[1,#], Xing-Zhen Liu[1,#], Jia Wang[2], Hai-Rong Tao[1], Tong Zhu[1], Wen-Jie Jin[1,*], Kang-Ping Shen[1,*]

1 Shanghai Key Laboratory of Orthopedic Implants, Department of Orthopedic Surgery, Shanghai Ninth People's Hospital, Shanghai Jiao Tong University School of Medicine, Shanghai, China

2 Department of Pathology, Shanghai Xinhua Hospital, Shanghai Jiao Tong University School of Medicine, Shanghai, China

Graphical Abstract

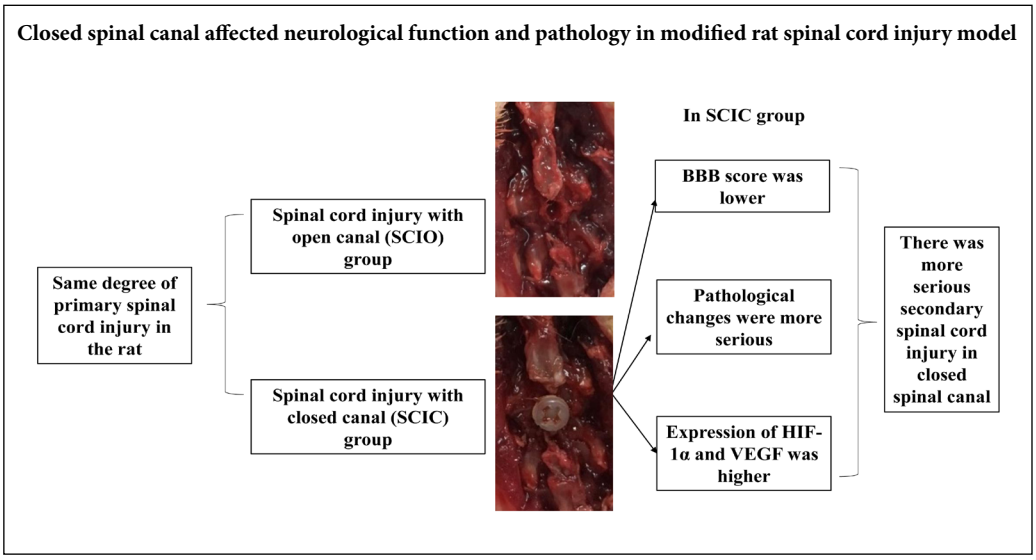

***Correspondence to:**
Wen-Jie Jin, MD, PhD, surgeonjin@126.com;
Kang-Ping Shen, MD, PhD, shkp2016@163.com.

#These two authors contributed equally to this paper.

orcid:
0000-0002-5521-7341 (Wen-Jie Jin)
0000-0003-4355-3142 (Kang-Ping Shen)

***doi:** 10.4103/1673-5374.266919*

***Received:** March 23, 2019*
***Peer review started:** March 28, 2019*
***Accepted:** May 9, 2019*
***Published online:** October 18, 2019*

Abstract

Most animal spinal cord injury models involve a laminectomy, such as the weight drop model or the transection model. However, in clinical practice, many patients undergo spinal cord injury while maintaining a relatively complete spinal canal. Thus, open spinal cord injury models often do not simulate real injuries, and few previous studies have investigated whether having a closed spinal canal after a primary spinal cord injury may influence secondary processes. Therefore, we aimed to assess the differences in neurological dysfunction and pathological changes between rat spinal cord injury models with closed and open spinal canals. Sprague-Dawley rats were randomly divided into three groups. In the sham group, the tunnel was expanded only, without inserting a screw into the spinal canal. In the spinal cord injury with open canal group, a screw was inserted into the spinal canal to cause spinal cord injury for 5 minutes, and then the screw was pulled out, leaving a hole in the vertebral plate. In the spinal cord injury with closed canal group, after inserting a screw into the spinal canal for 5 minutes, the screw was pulled out by approximately 1.5 mm and the flat end of the screw remained in the hole in the vertebral plate so that the spinal canal remained closed; this group was the modified model, which used a screw both to compress the spinal cord and to seal the spinal canal. At 7 days post-operation, the Basso-Beattie-Bresnahan scale was used to measure changes in neurological outcomes. Hematoxylin-eosin staining was used to assess histopathology. To evaluate the degree of local secondary hypoxia, immunohistochemical staining and western blot assays were applied to detect the expression of hypoxia-inducible factor 1α (HIF-1α) and vascular endothelial growth factor (VEGF). Compared with the spinal cord injury with open canal group, in the closed canal group the Basso-Beattie-Bresnahan scores were lower, cell morphology was more irregular, the percentage of morphologically normal neurons was lower, the percentages of HIF-1α- and VEGF-immunoreactive cells were higher, and HIF-1α and VEGF protein expression was also higher. In conclusion, we successfully established a rat spinal cord injury model with closed canal. This model could result in more serious neurological dysfunction and histopathological changes than in open canal models. All experimental procedures were approved by the Institutional Animal Care Committee of Shanghai Ninth People's Hospital, Shanghai Jiao Tong University School of Medicine, China (approval No. HKDL201810) on January 30, 2018.

***Key Words:** Basso-Beattie-Bresnahan scores; closed spinal canal; HIF-1α; hypoxia; model; nerve regeneration; open spinal canal; rat; secondary injury; spinal cord injury; VEGF*

***Chinese Library Classification No.** R447; R363; R364*

Introduction

Spinal cord injury (SCI) is one of the most important causes of severe disability worldwide, and can lead to permanent neurological dysfunction, costly health expenses, and large social burdens. It is reported that approximately 2.5 million individuals suffer from SCI, and more than 130,000 new SCIs occur every year (McLean, 2013; Dalbayrak et al., 2015; Jain et al., 2015). Therefore, the study of the pathophysiology of SCI, including primary and secondary injuries, is important to reduce neurological dysfunction (Oyinbo, 2011; Witiw and Fehlings, 2015; Ahuja et al., 2017a, b; Rouanet et al., 2017; Sweis and Biller, 2017; Cheng et al., 2019). Recently, many studies have focused on secondary SCI, and have reported that the secondary phase features a continuation of some of the events from the acute phase, such as electrolyte shifts, edema, and necrotic cell death, as well as some novel events, including the formation of free radicals, hypoxia, delayed calcium influx, inflammation, and apoptotic cell death (Oyinbo, 2011; Witiw and Fehlings, 2015; Ahuja et al., 2017a, b).

In the clinic, many patients undergo an SCI while maintaining a relatively complete spinal canal, such as in an SCI without radiological abnormality or a spinal cord contusion injury without fractures (Szwedowski and Walecki, 2014; Acker et al., 2016; Dixon, 2016; Asan, 2018; Atesok et al., 2018; Wang et al., 2019), and there is usually no obvious spinal cord compression caused by fractures and/or dislocation after primary SCI (Aito et al., 2007; Bracken, 2012; Jin et al., 2017). Therefore, secondary SCI in the complete spinal canal might affect the neurological recovery in those patients. Currently, most animal SCI models involve breaking the completeness of the spinal canal, such as in the water drop compression model, transection model, and semi-transection model. All of these animal models are different from the SCI with complete spinal canal that is commonly seen in clinical practice (Cheriyan et al., 2014; Forgione et al., 2014; Lukovic et al., 2015; Mondello et al., 2015). Laminectomy in these SCI models may reduce pressure in the spinal canal, thus further improving local blood circulation and relieving the pathophysiological processes of the secondary SCI (Cheriyan et al., 2014; Ramadan et al., 2017). However, little attention has been paid to whether or not it is necessary to use animal models with complete spinal canals to study secondary SCI. Therefore, we aimed to create an SCI model with a closed spinal canal in rats to further investigate the differences in neurological dysfunction and pathological changes between SCI models with open and closed spinal canals, and to study the possible mechanisms for these differences.

Materials and Methods

Animals

All experimental procedures were approved by the Institutional Animal Care Committee of Shanghai Ninth People's Hospital, Shanghai Jiao Tong University School of Medicine, China (HKDL201810) on January 30, 2018. Twenty-four healthy adult male Sprague-Dawley rats aged 10 months and weighing 500 g were obtained from the Animal Laboratory of Shanghai SLAC Co., Shanghai, China (animal license No. SCXK (Hu) 2012-0002). All rats were fed on a 12-hour light–dark cycle with water and food available ad libitum. The experimental procedure followed the United States National Institutes of Health Guide for the Care and Use of Laboratory Animals (NIH Publication No. 85-23, revised 1996).

Surgical approach and groups

All rats were intraperitoneally anesthetized with 3% sodium pentobarbital (1 mL/kg) and placed in a prone position. After sterilizing with povidone-iodine, skin preparation and sterile dressing were performed at the surgical thoracolumbar area. A 3 cm incision was cut in the middle of the thoracolumbar level. The skin and subcutaneous tissues were sequentially incised. The muscles around the spinous process–vertebral plate were bluntly dissected and the half spinous process of T9 was removed using a rongeur. The vertebral plate was drilled using Kirschner wire (diameter 1 mm). The tunnel was expanded with a flat Kirschner wire (diameter 1.5 mm). The flat screw (diameter 1.5 mm, length 3.5 mm) was then tapped using a screwdriver (the location of the inserting screw is shown in **Figure 1A**). During advancement of the flat screw, cortical somatosensory evoked potentials were monitored using an established method (Morris et al., 2013; Sun et al., 2016). Establishment of the model was considered successful when the amplitude was decreased to 25–30% of the normal range and the latency was prolonged < 10% (Sun et al., 2016). All rats were randomly divided into three groups. In the sham group (n = 8), the tunnel was expanded only, without inserting the screw into the spinal canal. In the SCI with open canal (SCIO) group (n = 8), after inserting the screw into the spinal canal to cause SCI for 5 minutes, the screw was pulled out, leaving a hole (Φ1.5 mm) in the vertebral plate. In the SCI with closed canal (SCIC) group (n = 8), the screw was inserted into the spinal canal for 5 minutes, and then the screw was pulled out approximately 1.5 mm, leaving the flat end of the screw in the hole of the vertebral plate to keep the spinal canal closed (**Figure 1B** and **C**). Preliminary tests showed that, in lateral X-rays of a 10-month-old rat, the sagittal diameter of the spinal canal was approximately 3.26 mm, and the sagittal diameter of the lamina was approximately 0.46 mm. Therefore, the flat end of the screw could be controlled to avoid invading the spinal canal space. Finally, the peripheral muscles and skin were sutured, and the wound was disinfected.

Electrophysiological monitoring during screw insertion

A sensory evoked potential device (Haishen, Shanghai, China) was connected to the rats (Morris et al., 2013; Sun et al., 2016). Briefly, the exciting electrodes were inserted into the fibular head subcutaneously, and one constant current pulse with a width of 0.2 ms and a frequency of 2.7 Hz was used to excite the tibial nerve. Another electrode was inserted subcutaneously into the skull to record evoked potentials. At a bandwidth of 2 to 2000 Hz, 200 cortical somatosensory evoked potentials were averaged and replicated. When the

screw was inserted in the spinal canal, cortical somatosensory evoked potentials were constantly monitored in all rats. The screwing process was stopped once the evoked potential amplitude was decreased to 25–30% of the normal range, and the latency was prolonged < 10%.

Examination time

According to previous studies, changes in neurological function, pathology, and the expression of hypoxia-inducible factor 1α (HIF-1α) and vascular endothelial growth factor (VEGF) reach a maximal level in the injured spinal cord at 7 days after SCI (Lonjon et al., 2010; Chen et al., 2013). Therefore, we chose 7 days post-operation to conduct the following examinations, including the Basso-Beattie-Bresnahan (BBB) scale score, hematoxylin-eosin staining, immunohistochemistry, and western blot assay.

BBB scale

A behavioral test for hind limb motor function was performed, and this was assessed using the BBB motor rating scale (Basso et al., 1995). This BBB scale was based on motor ability following SCI in a rat model. Briefly, the BBB scale is a 22-point scale from 0 to 21. Zero points indicate no observable hind limb movement, and 21 points indicate a sustained coordinated gait with consistent trunk stability and a parallel paw placement of the limbs. Two independent observers, blinded to the experiment, scored the locomotion, and the means of the two scores were calculated.

Hematoxylin-eosin staining

After examining neurological function, all rats were given intraperitoneal anesthesia (3% sodium pentobarbital, 1 mL/kg) and routinely sacrificed. Compressive spinal cord levels, showing a compressive imprint under the screw drill hole, were completely removed. Four randomly chosen specimens were fixed and kept in 4% paraformaldehyde overnight for post-fixation. After dehydration, the spinal cord was embedded in paraffin. Serial coronal sections were collected at 5 μm thickness, and five non-serial slices of each specimen were randomly selected for hematoxylin-eosin staining using well-established methods. Briefly, sections were stained with hematoxylin for 5 minutes followed by 5 dips in 1% acid ethanol (1% HCl in 70% ethanol) and then rinsed in distilled water. The sections were stained with eosin for 3 minutes, followed by dehydration in an alcohol gradient and clearing in xylene. Images were taken using an inverted microscope (Eclipse T3-S; Nikon, Tokyo, Japan) by two independent observers blinded to the experiment. All neurons were counted in each section of embedded spinal cord specimen. Morphologically normal neurons exhibited normal morphology, with uniformly stained cytoplasm and clear karyosomes. The percentage of morphologically normal neurons (%) was equal to the number of morphologically normal neurons/the total number of neurons. The mean number was obtained from counts by two observers.

Immunohistochemistry and image analysis

Five non-serial paraffin-embedded sections of the spinal cord were also subjected to immunohistochemical staining. Briefly, tissue sections of 5 μm were deparaffinized, rehydrated in a series of descending concentrations of ethanol, and underwent antigen retrieval (20 minutes of microwave irradiation in 0.1 M phosphate-buffered saline, pH 7.4). Endogenous peroxidases were blocked using 3% H_2O_2. After three rinses in phosphate-buffered saline for 5 minutes each, non-specific binding was blocked by incubating in 10% normal rabbit serum for 30 minutes at room temperature. Sections were then incubated with primary polyclonal HIF-1α antibody (1:800 dilution; Affinity Biosciences, Cincinnati, OH, USA) and primary polyclonal VEGF antibody (1:300 dilution; Affinity Biosciences) overnight at 4°C, followed by incubation with secondary goat anti-rabbit IgG (1:200 dilution; DAKO, Glostrup, Denmark) labeled with horseradish peroxidase at room temperature for 1 hour. Negative controls were used, in which IgGs replaced the primary antibody at an equal protein concentration. Immunoreactivity was visualized using the diaminobenzidine (DAB) chromogenic reagent (DAKO). Sections were counterstained with hematoxylin. Images were taken on an inverted microscope (Eclipse T3-S; Nikon) by two independent observers blinded to the experiment. All neurons were counted in each section of embedded spinal cord specimen. The percentage of HIF-1α- and VEGF-immunoreactive cells was equal to the number of immunoreactive cells/the total number of neurons, and mean scores were obtained from counts by two observers (Wang et al., 2014).

Western blot assay

Additional four specimens were used for western blotting. For protein sample collection, total injured spinal cord tissue was homogenized and extracted using RIPA buffer (Beyotime, Nanjing, China). Protein concentration was measured using a BCA protein assay kit (Beyotime) according to the manufacturer's instructions. Similar amounts of protein lysate (6 μL) were separated using a 10% sodium dodecyl sulfate polyacrylamide gel electrophoresis gel and transferred onto polyvinylidene fluoride (Millipore, Bedford, MA, USA) membranes. The polyvinylidene fluoride membranes were blocked with 5% fat-free powdered milk for 2 hours at room temperature. The membranes were then incubated with respective primary antibodies overnight at 4°C, which consisted of primary rabbit polyclonal HIF-1α antibody (1:1000 dilution; Affinity Biosciences), primary rabbit polyclonal VEGF antibody (1:1000 dilution; Affinity Biosciences), and β-actin (1:1000 dilution; Affinity Biosciences). After incubating with the secondary polyclonal goat anti-rabbit IgG (diluted 1:3000 in tris-buffered saline with Tween; Affinity Biosciences) at room temperature for one hour, the bands were observed using ECL plus reagent (THERMO, San Jose, CA, USA). Finally, the ratio of optical density values between HIF-1α, VEGF, and β-actin bands, which was used as an indicator of objective protein expression, was measured using AlphaEase FC software (Alpha Innotech, San Leandro,

CA, USA).

Statistical analysis

Statistical analysis was performed using SPSS software version 19.0 (IBM, Armonk, IL, USA). All results are represented as the mean ± SD. Intraoperative cortical somatosensory evoked potential outcomes, neurological outcomes, the percentage of morphologically normal neurons, and the percentage of HIF-1α- and VEGF-immunoreactive cells were analyzed using one-way analysis of variance followed by the Bonferroni correction in various groups. $P < 0.05$ was regarded as statistically significant.

Results

Cortical somatosensory evoked potential outcomes

As shown in **Figure 2**, there were no significant differences in evoked potential amplitudes and latencies between the SCIO and SCIC groups, indicating that the degree of primary injury was similar between the two groups.

Neurological outcomes

In the sham group, rats did not exhibit symptoms of neurological impairment following surgery, and the mean BBB score was 21. Rats showed various degrees of neurological dysfunction in the SCIC and SCIO groups. The BBB score was significantly lower in the SCIC group than in the SCIO group from 1 day to 7 days post-operation (**Figure 3**).

Histological outcomes

In the sham group, the morphology of the spinal cord was well maintained, and neurons exhibited normal morphology, with uniformly stained cytoplasm, clear karyosomes, and few vacuolar changes. In the SCIO group, the morphology of the spinal cord was irregular. The percentage of morphologically normal neurons was slightly decreased. Cell nuclei presented mild pyknosis, and vacuolization was apparent in the cytoplasm. In addition, the injured spinal cord exhibited glial proliferation. In the SCIC group, the morphology of the spinal cord was very irregular, and the percentage of morphologically normal neurons was markedly decreased. Cell nuclei presented obvious pyknosis, and the injured spinal cord exhibited obvious glial proliferation. The percentage of morphologically normal neurons was 79.65 ± 2.97% in the sham group, 49.64 ± 3.11% in the SCIO group, and 25.84 ± 1.84% in the SCIC group, respectively. There were significant differences between each of the groups ($P < 0.05$; **Figure 4**).

Immunohistochemical and western blot outcomes

Immunoreactive cells were stained yellow and could be observed in the spinal cord (**Figure 5**). Few immunoreactive cells were seen in the sham group. The percentage of HIF-1α-immunoreactive cells was 7.89 ± 1.65% in the sham group, 51.87 ± 2.82% in the SCIO group, and 64.73 ± 2.88% in the SCIC group, respectively; in addition, there were significant differences between each of the groups ($P < 0.05$). The percentage of VEGF-immunoreactive cells was 5.31 ± 1.17% in the sham group, 34.09 ± 1.85% in the SCIO group, and 44.17 ± 2.17% in the SCIC group, respectively; there were also significant differences between each of the groups ($P < 0.05$). The results of western blot assay also showed that HIF-1α and VEGF expression was increased in the SCIC group compared with the sham and SCIO groups (**Figure 6**).

Discussion

The results from tests of neurological function and histopathological changes in our study indicate a more serious degree of SCI in the SCIC group compared with the SCIO group, suggesting that a closed spinal canal might result in severe secondary SCI after the same degree of primary SCI. So far, several animal SCI models have been developed, and these can be classed into open laminectomy and closed compression models (Hashimoto and Fukuda, 1990; Lee et al., 2008; Cao et al., 2014; Cheriyan et al., 2014; Forgione et al., 2014; Lukovic et al., 2015; Mondello et al., 2015; Su et al., 2015; Cheng et al., 2016; Paterniti et al., 2018). Laminectomy models have been widely used in previous studies because they involve an easy operation and have good efficacy, but these models may not be suitable for studying SCI without spine fracture and/or dislocation, which is common in clinical practice (Cheriyan et al., 2014; Forgione et al., 2014; Lukovic et al., 2015; Mondello et al., 2015). Subsequently, some authors have described closed compression models of SCI without laminectomy, including balloon inflation and screw compression models; these can ensure the completeness of the spinal canal (Hashimoto and Fukuda, 1990; Purdy et al., 2003; Lee et al., 2008; Cao et al., 2014; Yang et al., 2017). Among these, the screw compression models, first described by Hashimoto in 1990, are popular for use in small animals, with the advantages of being a convenient operation that involves no radiation exposure and has a low experimental cost; however, this model is usually used to establish chronic SCI by gradually inserting the screw into the spinal canal (Hashimoto and Fukuda, 1990).

In the present study, a flat screw was used to establish a rat compression SCI model without laminectomy, and cortical somatosensory evoked potential monitoring was used to ensure reliable spinal cord compression. In contrast to animal SCI models with laminectomy, the insertion of the screw should be performed with great care to ensure the integrity of the lamina. In addition, too small animals are not suitable because their vertebral plates are easily broken. Furthermore, to accurately analyze secondary injuries and avoid the influence of the remaining screw on spinal canal volume in the SCIC group, we conducted a preliminary experiment to evaluate the relevant bone parameters before the present experiment was performed. Thus, we believe that the different results between the SCIO and SCIC groups might originate from secondary injury caused by a closed spinal canal.

Secondary SCI is always caused by spinal swelling, and the hemorrhaging of small blood vessels in the spinal canal. All of these factors can increase the intraspinal pressure in the limited space of the canal, which then reduces blood flow in the spinal cord, further resulting in local hypoxia (Leonard et al., 2015). Local hypoxia might lead to increased intracellular free Ca^{2+}, oxygen free radicals, mitochondrial dysfunc-

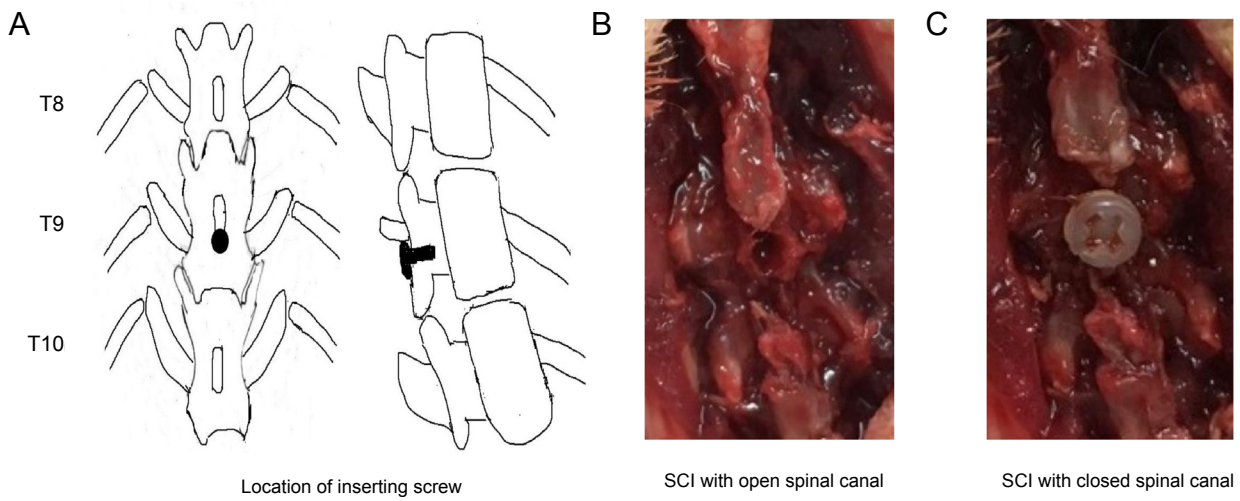

Figure 1 Rat screw compression SCI model.
(A) Location of screw insertion in the rat. After removing the half spinous process of T9, the vertebral plate was drilled and expanded with Kirschner wire before a flat screw (diameter 1.5 mm, length 3.5 mm) was inserted. (B) Rat SCI model with open spinal canal: After inserting the screw into the spinal canal, the screw was pulled entirely out. (C) Rat SCI model with closed spinal canal: After inserting the screw into the spinal canal, the screw was pulled out 1.5 mm, and the spinal canal was kept closed by the remaining screw. SCI: Spinal cord injury.

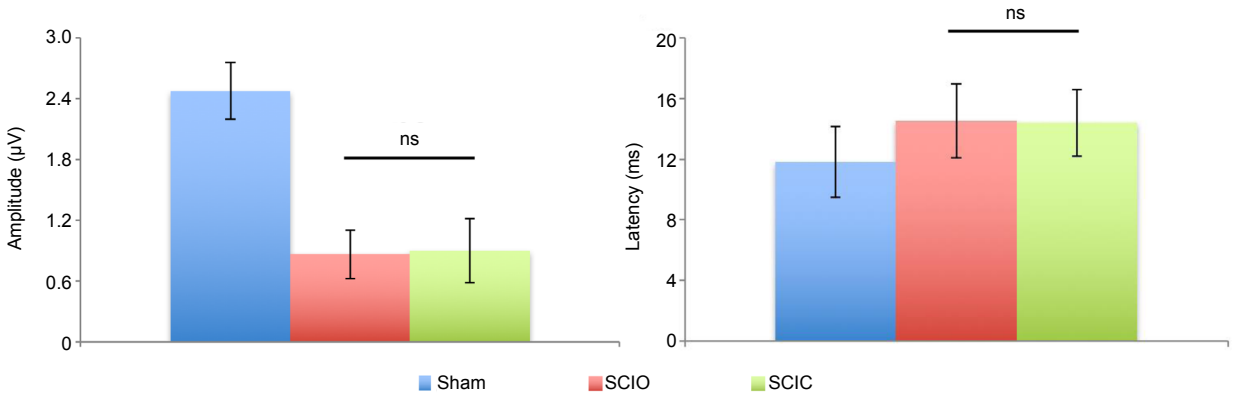

Figure 2 Results of intraoperative cortical somatosensory evoked potential monitoring.
The amplitudes and latencies were significantly decreased in the SCIO and SCIC groups compared with the sham group. There was no significant difference in amplitude and latency between the SCIO group and the SCIC group (mean ± SD, n = 8; one-way analysis of variance followed by the Bonferroni correction in various groups). $P > 0.05$. SCIO: Spinal cord injury with open canal; SCIC: spinal cord injury with closed canal; ns: not significant.

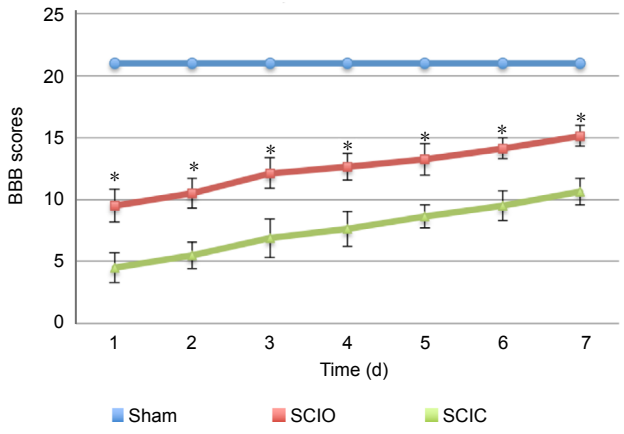

Figure 3 Influence of spinal canal environment on BBB scores after primary spinal cord injury in different groups, from 1 day to 7 days post-operation.
The rats in the sham group did not show symptoms of neurological impairment. The BBB score was significantly lower in the SCIC group than in the SCIO group (mean ± SD, n = 8; one-way analysis of variance followed by the Bonferroni correction in various groups).*P < 0.05, *vs.* SCIC group. BBB: Basso-Beattie-Bresnahan; SCIC: spinal cord injury with closed canal; SCIO: spinal cord injury with open canal.

tion, lysosomal damage, apoptosis, and immune inflammation damage, which would ultimately increase tissue injury and worsen functional outcomes (Oyinbo, 2011; Chen et al., 2013; Yang et al., 2013; Gurer et al., 2015; Saxena et al., 2015; Wang et al., 2016). Because the whole spinal canal is not completely closed, inflammatory reactions in the injured spinal cord can be metabolized by the circulation of cerebrospinal fluid through the spinal canal. However, the inflammatory reactions that are metabolized through the spinal canal may be relatively slow, leading to continuous high pressure and hypoxia in the injured spinal cord for a period of time. We hypothesize that, in the open model, decompression of the lamina at the site of the SCI may rapidly reduce intraspinal pressure at the injured spinal cord and quickly relieve local hypoxia. This may be the main reason why the BBB score was decreased in the SCIC group compared with the SCIO group at 1 day post-operation: because the secondary SCI might occur immediately after injury, and the corresponding symptoms of nerve injury may then occur within hours (Rajz et al., 2015; Raasck et al., 2017).

In the present study, HIF-1α and VEGF were used to indicate hypoxic changes after SCI (Greijer and van der Wall, 2004; Xiaowei et al., 2006; Ahluwalia and Tarnawski, 2012; Souvenir et al., 2014; Long et al., 2015). Previous studies have reported that the transcription and subsequent translation of HIF-1α and VEGF are increased under hypoxic conditions, further improving angiogenesis and correcting local circulation disorders (Greijer and van der Wall, 2004; Xiaowei et al., 2006; Ahluwalia and Tarnawski, 2012; Souvenir et al., 2014; Long et al., 2015; Wu et al., 2016). In our study, the expression of HIF-1α and VEGF was significantly higher in the SCIC group than in the SCIO group, indicating severe local hypoxia in the closed spinal canal after SCI.

There were some limitations to our study. First, we only compared the differences in neurological outcomes and histopathological changes between SCIC and SCIO groups, and preliminarily analyzed the characters of secondary SCI in these two groups, followed by a discussion of one possible mechanism: a hypoxic condition. However, further investigations should include a thorough study of the preliminary mechanisms and improve the standard of closed SCI models. Second, based on ethical demands, we only selected one time point to study, and subsequent research should be performed to add observational time points. Finally, if the BBB score of rats could be evaluated immediately after awakening from anesthesia and compared between the SCIO and SCIC groups, the severity of the primary SCI would be better reflected. However, because tolerance to anesthetics differed between rats, the awakening period was difficult to be defined, and further studies are required to address this problem.

In conclusion, the rat SCI model with closed spinal canal could result in more serious neurological dysfunction and histopathological changes compared with the open SCI model, and hypoxia may play a role in this process, at least to some extent. Thus, research into secondary SCI with a relatively completed canal could use this SCI model with closed canal to more accurately reflect clinical practice.

Author contributions: *Study design: WJJ, KPS; experimental implementation, data analysis: XS, XZL, JW, HRT, TZ; paper writing: XS, XZL, WJJ, KPS. All authors approved the final version of the paper.*
Conflicts of interest: *The authors declare that there are no conflicts of interest associated with this manuscript.*
Financial support: *None.*
Institutional review board statement: *All experimental procedures were approved by the Institutional Animal Care Committee of Shanghai Ninth People's Hospital, Shanghai Jiao Tong University School of Medicine, China (approval No. HKDL201810) on January 30, 2018.*
Copyright license agreement: *The Copyright License Agreement has been signed by all authors before publication.*
Data sharing statement: *Datasets analyzed during the current study are available from the corresponding author on reasonable request.*
Plagiarism check: *Checked twice by iThenticate.*
Peer review: *Externally peer reviewed.*

References

Acker G, Schneider UC, Grozdanovic Z, Vajkoczy P, Woitzik J (2016) Cervical disc herniation as a trigger for temporary cervical cord ischemia. J Spine Surg 2:135-138.

Ahluwalia A, Tarnawski AS (2012) Critical role of hypoxia sensor-HIF-1alpha in VEGF gene activation. Implications for angiogenesis and tissue injury healing. Curr Med Chem 19:90-97.

Ahuja CS, Wilson JR, Nori S, Kotter MRN, Druschel C, Curt A, Fehlings MG (2017a) Traumatic spinal cord injury. Nat Rev Dis Primers 3:17018.

Ahuja CS, Nori S, Tetreault L, Wilson J, Kwon B, Harrop J, Choi D, Fehlings MG (2017b) Traumatic spinal cord injury-repair and regeneration. Neurosurgery 80:S9-S22.

Aito S, D'Andrea M, Werhagen L, Farsetti L, Cappelli S, Bandini B, Di Donna V (2007) Neurological and functional outcome in traumatic central cord syndrome. Spinal Cord 45:292-297.

Asan Z (2018) Spinal cord injury without radiological abnormality in adults: clinical and radiological discordance. World Neurosurg 114:e1147-1151.

Atesok K, Tanaka N, O'Brien A, Robinson Y, Pang D, Deinlein D, Manoharan SR, Pittman J, Theiss S (2018) Posttraumatic spinal cord injury without radiographic abnormality. Adv Orthop 2018:7060654.

Basso DM, Beattie MS, Bresnahan JC (1995) A sensitive and reliable locomotor rating scale for open field testing in rats. J Neurotrauma 12:1-21.

Bracken MB (2012) Steroids for acute spinal cord injury. Cochrane Database Syst Rev 1:Cd001046.

Cao P, Zheng Y, Zheng T, Sun C, Lu J, Rickett T, Shi R (2014) A model of acute compressive spinal cord injury with a minimally invasive balloon in goats. J Neurol Sci 337:97-103.

Chen MH, Ren QX, Yang WF, Chen XL, Lu C, Sun J (2013) Influences of HIF-1α on Bax/Bcl-2 and VEGF expressions in rats with spinal cord injury. Int J Clin Exp Pathol 6:2312-2322.

Cheng I, Githens M, Smith RL, Johnston TR, Park DY, Stauff MP, Salari N, Tileston KR, Kharazi AI (2016) Local versus distal transplantation of human neural stem cells following chronic spinal cord injury. Spine J 16:764-769.

Cheng JP, Li H, Li XJ (2019) Bone marrow mesenchymal stem cell transplantation combined with Lindera glauca leaf extract attenutes inflammation after spinal cord injury. Zhongguo Zuzhi Gongcheng Yanjiu 23:1975-1981.

Cheriyan T, Ryan DJ, Weinreb JH, Cheriyan J, Paul JC, Lafage V, Kirsch T, Errico TJ (2014) Spinal cord injury models: a review. Spinal Cord 52:588-595.

Dalbayrak S, Yaman O, Yilmaz T (2015) Current and future surgery strategies for spinal cord injuries. World J Orthop 6:34-41.

Dixon A (2016) Cervical spinal injury in pediatric blunt trauma patients: management in the emergency department. Pediatr Emerg Med Pract 13:1-24.

Forgione N, Karadimas SK, Foltz WD, Satkunendrarajah K, Lip A, Fehlings MG (2014) Bilateral contusion-compression model of incomplete traumatic cervical spinal cord injury. J Neurotrauma 31:1776-1788.

Greijer AE, van der Wall E (2004) The role of hypoxia inducible factor 1 (HIF-1) in hypoxia induced apoptosis. J Clin Pathol 57:1009-1014.

Gurer B, Kertmen H, Kasim E, Yilmaz ER, Kanat BH, Sargon MF, Arikok AT, Erguder BI, Sekerci Z (2015) Neuroprotective effects of testosterone on ischemia/reperfusion injury of the rabbit spinal cord. Injury 46:240-248.

Hashimoto T, Fukuda N (1990) New spinal cord injury model produced by spinal cord compression in the rat. J Pharmacol Methods 23:203-212.

Jain NB, Ayers GD, Peterson EN, Harris MB, Morse L, O'Connor KC, Garshick E (2015) Traumatic spinal cord injury in the United States, 1993-2012. JAMA 313:2236-2243.

Jin W, Sun X, Shen K, Wang J, Liu X, Shang X, Tao H, Zhu T (2017) Recurrent neurological deterioration after conservative treatment for acute traumatic central cord syndrome without bony injury: seventeen operative case reports. J Neurotrauma 34:3051-3057.

Lee JH, Choi CB, Chung DJ, Kang EH, Chang HS, Hwang SH, Han H, Choe BY, Sur JH, Lee SY, Kim HY (2008) Development of an improved canine model of percutaneous spinal cord compression injury by balloon catheter. J Neurosci Methods 167:310-316.

Leonard AV, Thornton E, Vink R (2015) The relative contribution of edema and hemorrhage to raised intrathecal pressure after traumatic spinal cord injury. J Neurotrauma 32:397-402.

Long HQ, Li GS, Cheng X, Xu JH, Li FB (2015) Role of hypoxia-induced VEGF in blood-spinal cord barrier disruption in chronic spinal cord injury. Chin J Traumatol 18:293-295.

Lonjon N, Kouyoumdjian P, Prieto M, Bauchet L, Haton H, Gaviria M, Privat A, Perrin FE (2010) Early functional outcomes and histological analysis after spinal cord compression injury in rats. J Neurosurg Spine 12:106-113.

Lukovic D, Moreno-Manzano V, Lopez-Mocholi E, Rodriguez-Jimenez FJ, Jendelova P, Sykova E, Oria M, Stojkovic M, Erceg S (2015) Complete rat spinal cord transection as a faithful model of spinal cord injury for translational cell transplantation. Sci Rep 5:9640.

McLean AN (2013) The spinal cord-injured patient in the medical ward. Clin Med (Lond) 13:549-552.

Mondello SE, Sunshine MD, Fischedick AE, Moritz CT, Horner PJ (2015) A cervical hemi-contusion spinal cord injury model for the investigation of novel therapeutics targeting proximal and distal forelimb functional recovery. J Neurotrauma 32:1994-2007.

Morris SH, El-Hawary R, Howard JJ, Rasmusson DD (2013) Validity of somatosensory evoked potentials as early indicators of neural compromise in rat model of spinal cord compression. Clin Neurophysiol 124:1031-1036.

Oyinbo CA (2011) Secondary injury mechanisms in traumatic spinal cord injury: a nugget of this multiply cascade. Acta Neurobiol Exp (Wars) 71:281-299.

Paterniti I, Esposito E, Cuzzocrea S (2018) An in vivo compression model of spinal cord injury. Methods Mol Biol 1727:379-384.

Purdy PD, Duong RT, White CL 3rd, Baer DL, Reichard RR, Pride GL Jr., Adams C, Miller S, Hladik CL, Yetkin Z (2003) Percutaneous translumbar spinal cord compression injury in a dog model that uses angioplasty balloons: MR imaging and histopathologic findings. AJNR Am J Neuroradiol 24:177-184.

Raasck K, Habis AA, Aoude A, Simoes L, Barros F, Reindl R, Jarzem P (2017) Spontaneous spinal epidural hematoma management: a case series and literature review. Spinal Cord Ser Cases 3:16043.

Rajz G, Cohen JE, Harnof S, Knoller N, Goren O, Shoshan Y, Fraifeld S, Kaplan L, Itshayek E (2015) Spontaneous spinal epidural hematoma: the importance of preoperative neurological status and rapid intervention. J Clin Neurosci 22:123-128.

Ramadan WS, Abdel-Hamid GA, Al-Karim S, Abbas AT (2017) Histological, immunohistochemical and ultrastructural study of secondary compressed spinal cord injury in a rat model. Folia Histochem Cytobiol 55:11-20.

Rouanet C, Reges D, Rocha E, Gagliardi V, Silva GS (2017) Traumatic spinal cord injury: current concepts and treatment update. Arq Neuropsiquiatr 75:387-393.

Saxena T, Loomis KH, Pai SB, Karumbaiah L, Gaupp E, Patil K, Patkar R, Bellamkonda RV (2015) Nanocarrier-mediated inhibition of macrophage migration inhibitory factor attenuates secondary injury after spinal cord injury. ACS Nano 9:1492-1505.

Souvenir R, Flores JJ, Ostrowski RP, Manaenko A, Duris K, Tang J (2014) Erythropoietin inhibits HIF-1 alpha expression via upregulation of PHD-2 transcription and translation in an in vitro model of hypoxia-ischemia. Transl Stroke Res 5:118-127.

Su YF, Lin CL, Lee KS, Tsai TH, Wu SC, Hwang SL, Chen SC, Kwan AL (2015) A modified compression model of spinal cord injury in rats: functional assessment and the expression of nitric oxide synthases. Spinal Cord 53:432-435.

Sun Y, Zhang LH, Fu YM, Li ZR, Liu JH, Peng J, Liu B, Tang PF (2016) Establishment of a rat model of chronic thoracolumbar cord compression with a flat plastic screw. Neural Regen Res 11:963-970.

Sweis R, Biller J (2017) Systemic complications of spinal cord injury. Curr Neurol Neurosci Rep 17:8.

Szwedowski D, Walecki J (2014) Spinal cord injury without radiographic abnormality (SCIWORA)-clinical and radiological aspects. Pol J Radiol 79:461-464.

Wang J, Guo S, Cai X, Xu JW, Li HP (2019) Establishment and verification of a surgical prognostic model for cervical spinal cord injury without radiological abnormality. Neural Regen Res 14:713-720.

Wang X, Li J, Wu D, Bu X, Qiao Y (2016) Hypoxia promotes apoptosis of neuronal cells through hypoxia-inducible factor-1alpha-microRNA-204-B-cell lymphoma-2 pathway. Exp Biol Med (Maywood) 241:177-183.

Wang Y, Liu CF, Wang QP, Gao H, Na HR, Yu RT (2014) Establishment of a spinal cord injury model in adult rats by an electrocircuit-controlled impacting device and its pathological observations. Cell Biochem Biophys 69:333-340.

Witiw CD, Fehlings MG (2015) Acute spinal cord injury. J Spinal Disord Tech 28:202-210.

Wu J, Ke X, Fu W, Gao X, Zhang H, Wang W, Ma N, Zhao M, Hao X, Zhang Z (2016) Inhibition of hypoxia-induced retinal angiogenesis by specnuezhenide, an effective constituent of ligustrum lucidum ait., through suppression of the HIF-1 alpha/VEGF signaling pathway. Molecules 21:E1756.

Xiaowei H, Ninghui Z, Wei X, Yiping T, Linfeng X (2006) The experimental study of hypoxia-inducible factor-1alpha and its target genes in spinal cord injury. Spinal Cord 44:35-43.

Yang C, Yu B, Ma F, Lu H, Huang J, You Q, Yu B, Qiao J, Feng J (2017) What is the optimal sequence of decompression for multilevel non-continuous spinal cord compression injuries in rabbits? BMC Neurol 17:44.

Yang SH, Gangidine M, Pritts TA, Goodman MD, Lentsch AB (2013) Interleukin 6 mediates neuroinflammation and motor coordination deficits after mild traumatic brain injury and brief hypoxia in mice. Shock 40:471-475.

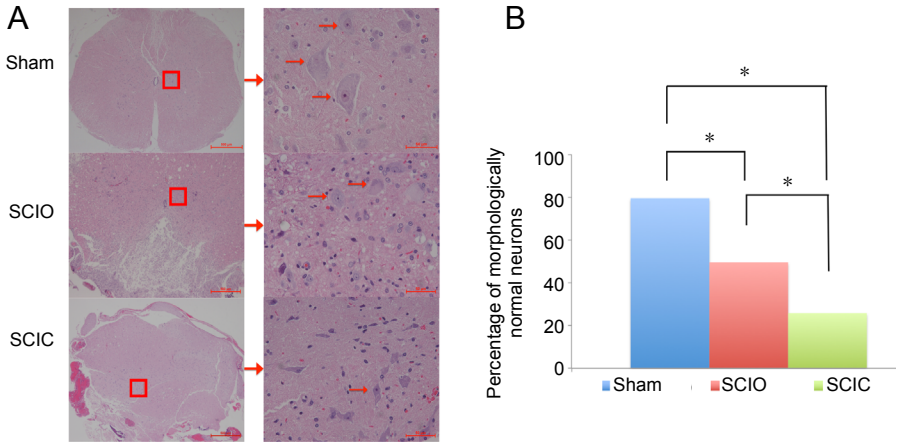

Figure 4 Influence of spinal canal environment on histological changes after primary spinal cord injury in different groups at 7 days post-operation.
(A) Hematoxylin-eosin staining: In the sham group, there were no obvious histological changes. Typical changes in neurons are marked by arrows. In the SCIO group, there was mildly irregular morphology, decreased numbers of morphologically normal neurons, and nuclei pyknosis. In the SCIC group, there was severe irregular morphology, markedly decreased numbers of morphologically normal neurons, and obvious nuclei pyknosis. Scale bars: 500 μm (left) and 50 μm (right). (B) Percentages of morphologically normal neurons in the injured spinal cord. The percentage of morphologically normal neurons was lower in the SCIC group than in the SCIO group (∗$P < 0.05$; mean ± SD, $n = 8$; one-way analysis of variance followed by the Bonferroni correction in various groups). SCIC: Spinal cord injury with closed canal; SCIO: spinal cord injury with open canal.

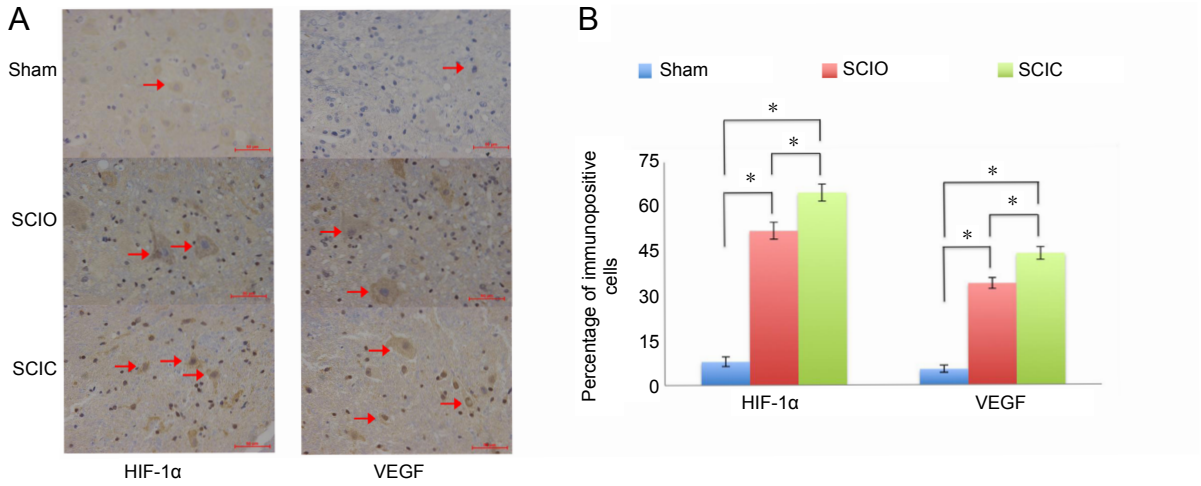

Figure 5 Influence of spinal canal environment on changes in immunohistochemical staining after primary spinal cord injury in different groups at 7 days post-operation.
(A) Immunohistochemical staining: The immunoreactive cells were stained yellow and observed in the spinal cord. Typical immunoreactive cells are marked by arrows. Few immunoreactive cells were seen in the sham group, and the number of immunoreactive cells was higher in the SCIC group than in the SCIO group. Scale bars: 500 μm. (B) Percentage of immunoreactive cells in the injured spinal cord: The percentages of HIF-1α- and VEGF-immunoreactive cells were higher in the SCIC group than in the SCIO group (∗$P < 0.05$; mean ± SD, $n = 8$; one-way analysis of variance followed by the Bonferroni correction in various groups). HIF-1α: Hypoxia-inducible factor 1α; SCIC: spinal cord injury with closed canal; SCIO: spinal cord injury with open canal; VEGF: vascular endothelial growth factor.

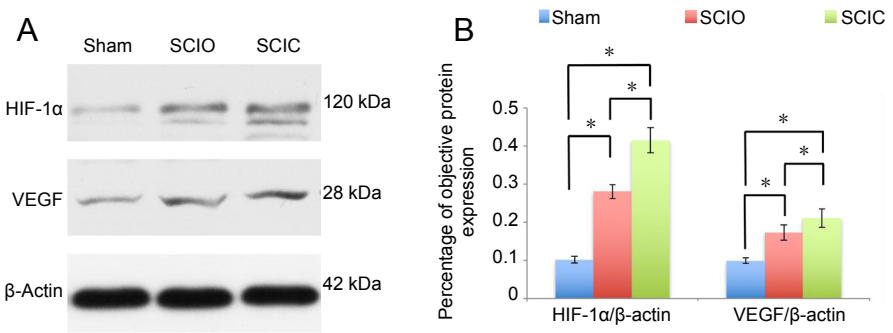

Figure 6 Influence of spinal canal environment on western blot results after primary spinal cord injury in different groups at 7 days post-operation.
(A) Western blot bands: The bands were more obvious in the SCIC group than in the SCIO group. (B) Percentage of objective protein expression in the injured spinal cord. The expression of HIF-1α and VEGF proteins was higher in the SCIC group than in the SCIO group (∗$P < 0.05$; mean ± SD, $n = 8$; one-way analysis of variance followed by the Bonferroni correction in various groups). HIF-1α: Hypoxia-inducible factor 1α; SCIC: spinal cord injury with closed canal; SCIO: spinal cord injury with open canal; VEGF: vascular endothelial growth factor.

C-Editor: Zhao M; S-Editors: Wang J, Li CH; L-Editors: Bonnie, Robens J, Qiu Y, Song LP; T-Editor: Jia Y